JOURNAL OF EXPERIMENTAL AND THEORETICAL PHYSICS, 2024, Vol. 165, No. 2, pp. 247–254

ORDER, DISORDER, AND PHASE TRANSITION IN CONDENSED MEDIA

COLLAPSE OF MINOR MAGNETIC HYSTERESIS LOOP IN GRANULAR HIGH-T_C SUPERCONDUCTOR $YBa_2Cu_3O_{7-\delta}$

© 2024 D.A. Balaev*, S.V. Semenov, D. M. Gokhfeld, M. I. Petrov

Kirensky Institute of Physics, Krasnoyarsk Scientific Center, Siberian Branch of the Russian Academy of Sciences, Krasnoyarsk 660036, Russia

**e-mail: dabalaev@iph.krasn.ru*

Received September 12, 2023

Revised October 13, 2023

Accepted October 16, 2023

Abstract. The evolution of the magnetic hysteresis loops of the granular high-temperature superconductor $YBa_2Cu_3O_{7-\delta}$ with varying the maximum external applied field H_{max} has been experimentally studied. In the range of weak fields (up to ~10 Oe at a temperature of 78 K), the small hysteresis loop is observed, associated with diamagnetism and the penetration of Josephson vortices into the subsystem of intergranular boundaries, which is a Josephson medium. With further growth of H_{max}, the larger magnetization hysteresis loop appears, associated with the penetration of Abrikosov vortices into superconducting granules. When analyzing the experimental data, a non-trivial fact was discovered: the magnetic response from the subsystem of intergranular boundaries becomes less noticeable with increasing H_{max}, and at a certain value of H_{max} this response disappears. This occurs even though the small hysteresis loop at small values of H_{max} is comparable to the magnetic response of superconducting granules.

The described evolution of magnetic hysteresis is explained using the concept of an effective field in an intergranular medium. The total magnetic field in the subsystem of intergranular boundaries is determined not only by the external field, but also by closing fields from the magnetic moments of superconducting granules. In other words, the interaction between the superconducting subsystems of granules and intergranular boundaries leads to the small hysteresis loop in sufficiently small fields, and to its complete disappearance with increasing magnetization modulus of superconducting granules.

Keywords: *Granular HTS*, *YBCO*, *effective field in the intergrain medium*, *magnetization hysteresis*, *trapped magnetic flux*, *Abrikosov vortex*, *Josephson vortex*

DOI: 10.31857/S00444510240211e7

1. INTRODUCTION

The parameters of the magnetic hysteresis loop are one of the main characteristics of superconductors both for practical applications and for understanding the fundamental processes of penetration, distribution, and anchoring (pinning) of Abrikosov vortices. The diversity of types of superconducting materials [1-6] and the need for controlled control of vortex pinning [7, 8] require an understanding of the physical mechanisms of the formation of magnetization hysteresis loops, which has prompted numerous studies [9-24]. In the almost 60 years since the Bean critical state model [25] appeared, there have been many further modifications, improvements, and changes, see, for example, [26], including those that take into account the granularity of the superconducting material [27-31].

The granular structure of high-temperature superconductors (HTS) and their small coherence length cause that the transfer of superconducting current through the intergranular boundaries occurs due to the Josephson effect. The subsystem of intergranular boundaries is a network of Josephson junctions and is a separate "weak" superconducting subsystem connected with another already "strong" superconducting subsystem – HTS granules. As a result, a two-level superconducting state is formed in granular HTS materials [27], which is manifested in their magnetic-transport properties, such as the two-step transition to the superconducting state observed in the resistance

dependences on temperature in an external field, or stepped character of magnetoresistance (at constant temperature).

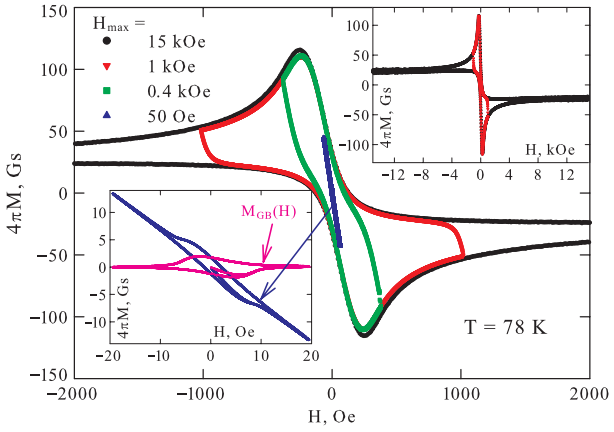

Fig 1. Magnetic hysteresis loops $M(H)$ of the studied sample $YBa_2Cu_3O_{7-\delta}$ in different external field ranges. The legend corresponds to both the main figure and the insets. The lower inset shows the contribution from the $M_{GB}(H)$ intergranular boundary subsystem obtained after subtracting the field linear diamagnetic contribution from the superconducting granules.

The subsystems of intergranular boundaries and granules are also characterized by the presence of hysteresis in different ranges of magnetic fields [32-35]. It should be noted that the vast majority of studies consider magnetization hysteresis in moderate and strong magnetic fields, where the magnetic response is mainly determined by superconducting granules. At the same time, little attention has been paid to the hysteresis behavior of magnetization associated with the intergranular boundary subsystem (hereafter referred to as small hysteresis), and the aforementioned papers [32-35] are a very representative list of works on this topic. In this work, we set out to investigate in detail the evolution of the magnetic hysteresis shape of the granular Y-Ba-Cu-O HTS system under increasing external field and to reveal the peculiarities of the interaction and mutual influence of the subsystems of intergranular boundaries and superconducting granules.

2. EXPERIMENT

The $YBa_2Cu_3O_{7-\delta}$ HTS sample was prepared by solid-phase synthesis in air atmosphere from the corresponding oxides with three intermediate grindings. At the final stage of preparation, special measures were taken to optimize the annealing (50h at 940°C followed by holding at 350°C for 10h).

Only reflections corresponding to the 1-2-3 structure were present on the diffractogram. The average size of granules according to scanning electron microscopy was about 10 μm. The temperature of the transition to the superconducting state according to magnetic and transport (onset of transition) measurements was 93 K, the value of the critical current at the temperature of liquid nitrogen was 150 A/cm^2.

Magnetic measurements were carried out on a LakeShore VSM 8604 vibrating magnetometer. For measurements the sample was made in the form of a ball with a diameter of about 3 mm. The magnetic hysteresis loops were measured at 78 K. The rate of field variation was 0.1-10 Oe/s (for the small and large field ranges, respectively). The experimental data (external field magnitude) were corrected for the demagnetizing factor of the sample.

3. RESULTS AND DISCUSSION

The general form of the $M(H)$ dependences in the field range up to ±15 kOe and also up to ±1 kOe is shown in the upper inset of Fig. 1. The asymmetric form of the $M(H)$ dependences with respect to the abscissa axis is typical for granular HTSs at sufficiently high temperatures. This asymmetry is explained by the presence of a surface layer in the granules in which the pinning of Abrikosov's vortices is weakened [30, 31, 36-38]. The mutual arrangement of the $M(H)$ dependences measured to different values of the maximum applied field, including $H_{max} = \pm 50$ Oe, is shown in Fig. 1 (main figure). Note that all dependencies in Fig. 1 are measured after cooling at zero external field. The behavior of the $M(H)$ dependence measured in the range of small fields (±50 Oe) in the vicinity of the origin is shown in the bottom inset of Fig. 1. It follows from these data that in the field range up to about 12 Oe, the $M(H)$ dependence exhibits hysteresis, while further, with increasing external field, the magnetization behaves in an almost reversible manner and the $M(H)$ dependence is linear in the field.

The described small hysteresis, clearly visible in the lower inset of Fig. 1, is the response of the intergranular boundary subsystem, as discussed in the Introduction and observed in the papers cited above [32-35]. It should also be noted here that small hysteresis is not observed on the grinded (from pellets) to powder HTS samples. The diamagnetic response from superconducting pellets is observed as a field linear and almost reversible behavior of the $M(H)$ dependence in fields larger than about 10 Oe. By subtracting this linear

contribution χH (where $\chi < 0$) from the experimental $M(H)$ dependence, the hysteresis loop of the $M_{GB}(H)$ magnetization from the intergranule boundary subsystem can be obtained:

$$M_{GB}(H) = M(H) - \chi H.$$

The obtained hysteresis dependence of $M_{GB}(H)$ is shown in the lower inset of Fig. 1. It is similar to the hysteresis loops of the magnetization of superconductors of the second kind (the subsystem of intergranular boundaries, i.e., the Josephson medium, is a superconductor of the second kind [39, 40]).

The critical state model [25] establishes the relationship between the magnetization and the critical current density J_C, which makes it possible to determine J_C from magnetic measurements. For an infinitely long cylinder with diameter d [31]

$$J_C(A/\mathrm{cm}^2) = 30\,\Delta\mathrm{M}[CGSM\ un./\mathrm{cm}^3]\,/\,d[cm], \quad (1)$$

where ΔM is the height of the magnetization hysteresis loop, $\Delta M(H) = M_{dec}(H) - M_{inc}(H)$, $M_{inc}(H)$ and $M_{dec}(H)$ are the hysteresis branches for increasing and decreasing external field, respectively. For a ball-shaped sample, such a simple analytical expression (Bean's formula) gives only an approximate value. A more accurate approximation for estimating J_C in a ball-shaped sample can be obtained by replacing d by the effective value $d_{eff} = \pi d_{circle}/4$, where d_{circle} is the diameter of the ball. The value of ΔM at $H \approx 0$ is 0.24 units SGSM/cm^3 and $d_{eff} = 0.131$ cm, giving $J_{CGB} = 55$ A/cm^2 . It is well known that Bean's formula gives underestimated values of the critical current near $H = 0$ [41-44]. Indeed, the value of the critical current determined from transport measurements by the four-probe method is somewhat higher (~ 150 A/cm^2).

For the magnetic hysteresis loop measured to fields larger than 1 kOe, it is necessary to substitute in expression (1) not the sample size, but the average size of the granules [45], since the intergranular currents are suppressed in large fields. For a large loop, we obtain the value of the intragranular critical current $J_{CG} \sim 2 \cdot 10^5$ A/cm^2 at $d \sim 10$ μm. The described difference of several orders of magnitude in the values of J_{CGB} and J_{CG} is a characteristic feature of granular HTSs. In the light of the above, for the complete magnetic hysteresis loop $M_{total}(H)$ (below we will use the notation $M(H)$, $M_{total}(H) \equiv M(H)$) of a granular superconductor can be written down in the following expression:

$$M(H) = M_{GB}(H) + M_G(H), \quad (2)$$

where $M_G(H)$ is the response from superconducting granules. The additive contribution from the two contributions to the total magnetization of the granular sample was implied in a number of studies cited above. However, expression (2) lacks the relationship between the intergranular boundary and granule subsystems. To elucidate such a relationship, the partial hysteresis loops of the magnetization were measured with successive increases in the maximum applied field $\pm H_{max}$. These data are summarized in Fig. 2. The step along the increasing maximum field value was (taking into account the demagnetizing factor of the sample)10-13 Oe.

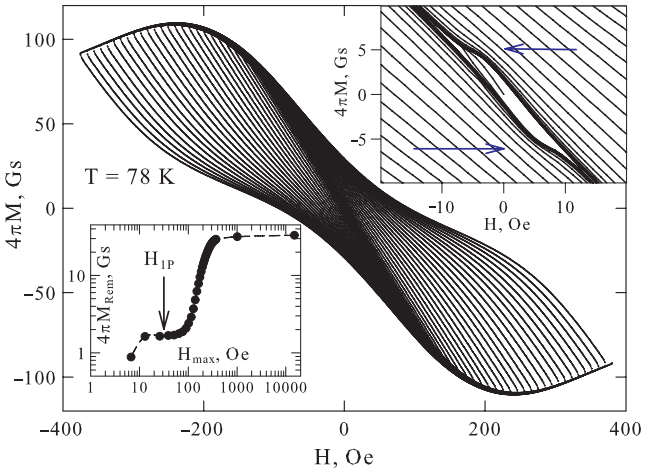

Fig. 2. Magnetization hysteresis loops obtained at different values of the maximum applied field $\pm H_{max}$ with successive increase of the H_{max} value. The upper inset shows the same loops in the vicinity of the origin on an enlarged scale; the arrows point to the discussed arc-shaped feature. The lower inset shows the dependence of the residual magnetization M_{Rem} ($H_{dec} = 0$) on H_{max} in double logarithmic scale.

Let us first focus on the behavior of the residual magnetization M_{Rem} as a function of H_{max}, shown in the lower inset of Fig. 2 (double logarithmic scale used). This dependence has a two-step character, in which there is an intermediate saturation (in fields larger than about 10 Oe) and another (main) saturation in larger fields. The departure from a roughly constant value at the intermediate saturation occurs at a field of about 35-40 Oe, as indicated (arrow) in the lower inset of Fig. 2. Obviously, in this interval of the external fields, the penetration of Abrikosov vortices inside the granules begins, and this field is called the field of the first penetration of H_{1P} [34, 35, 46, 47]. Consequently, at $H_{max} \geqslant H_{1P}$, we deal with the superposition of two hysteresis magnetizations from two subsystems

(intergranular boundaries and granules), according to expression (2).

In the form of partial hysteresis loops in the origin region, the arch-shaped features (curving), clearly visible in the enlarged scale in the upper inset of Fig. 2 (marked with horizontal arrows), attract attention. These bends of the $M(H_{inc})$ and $M(H_{dec})$ dependences are observed in the vicinity of the field of about ±5 Oe, and they are associated with the contribution from small hysteresis (the presence of extrema of the $M_{GB}(H)$ dependence, see the lower inset of Fig. 1). At the same time, from the data shown in the upper inset of Fig. 2, we can conclude that at sufficiently large values of H_{max} the described feature becomes either weakly pronounced or absent. In other words, in a certain range of H_{max} values the influence of small hysteresis is preserved, and at sufficiently large values of H_{max} the contribution from magnetic hysteresis becomes insignificant. The described behavior is illustrated in more detail in Fig. 3a, which shows the plots of $M(H)$ dependences when the external field changes from $+H_{max}$ to $-H_{max}$ for values of H_{max} in the range from 13 to 184 Oe. The shape of the discussed feature on the $M(H)$ dependence in the form of an arch implies two alternate changes of the curvature sign when the field changes; the field at which the curvature sign changes is indicated in Fig. 3*a* by arrows. In the absence of the arch-shaped feature, there is no change in the sign of curvature and the dependence $M(H)$ is, to a first approximation, a linear function (in Fig. 3*a*, straight lines are drawn to compare with the experimental data at H_{max} = 162, 173, and 184 Oe). Figures 3*b*, 3*c* illustrate the derivatives $dM(H)/dH$. At sufficiently small values of H_{max}, the dM/dH derivatives show two distinct extrema, which become weakly pronounced as H_{max} increases. From analyzing the data in Fig. 3*b*, 3*c* we can conclude that at H_{max} = 173 Oe there are no extrema on the dM/dH derivatives, and the $M(H)$ dependences in the range +20 to –20 Oe are almost linear functions relative to the field (see Fig. 3*a*). Thus, at values of the maximum applied field around 173 Oe and large values of H_{max}, the small hysteresis of magnetization does not manifest itself in the region of small fields.

The range of variation of the ΔM_{GB} small hysteresis magnetization ($M_{GB}(H)$ dependence) in the ±10 Oe range is about 2 G (see the bottom inset of Fig. 1), while the magnitude of the total magnetization at H_{max} = 173 Oe in the ±10 Oe neighborhood varies from 5 to 15 G (Fig. 3*a*). Thus, ΔM_{GB} and $M(H = \pm 10$ Oe) are comparable values. The absence of the manifestation of an extremum from small hysteresis on the $M(H)$ dependence at sufficiently large

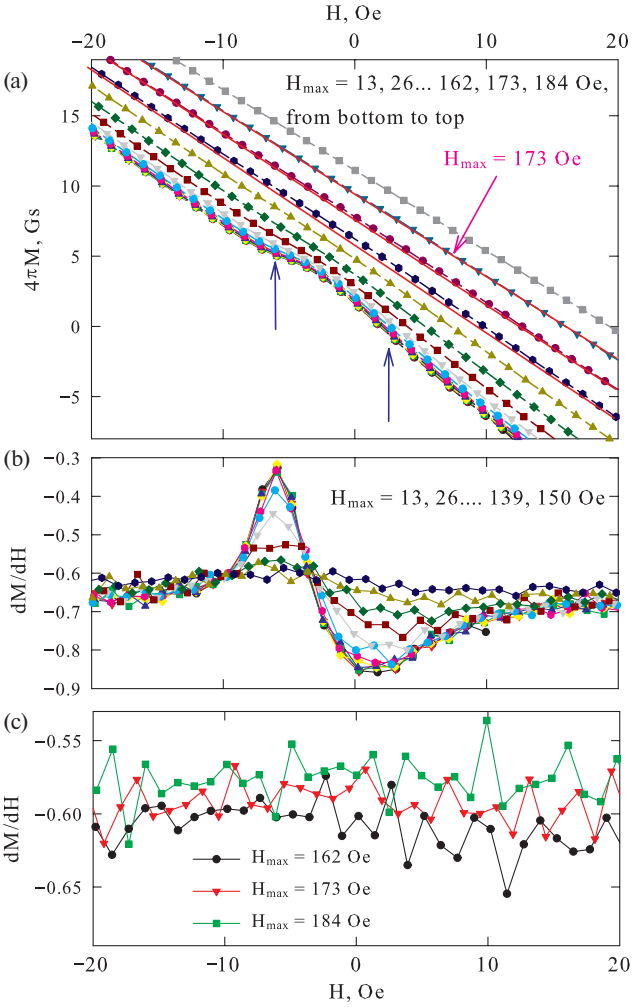

Fig. 3. *a* – plots of $M(H)$ dependences (from the data of Fig. 2) in the range ±20 Oe at change of the external field H from $+H_{max}$ to $-H_{max}$ (symbols); straight lines – approximation by a linear function, *b*, *c* – derivatives of dM/dH for the data shown in Fig. *a*.

values of H_{max} means that the contribution from small hysteresis is not always additive to the contribution from superconducting granules. The observed fact, i.e., collapse of the small magnetic hysteresis loop, to the best of our knowledge, has not been revealed in early studies [32-35]. To explain the behavior of the small loop, it is necessary to take into account the interaction between the granule subsystems and intergranular boundaries. Instead of expression (2), we can formally write as follows

$$M(H) = M_{GB}(H, M_G(H)) + M_G(H), \qquad (3)$$

implying that M_{GB} decreases both with increasing H and with increasing M_G. In other words, the intergranular medium is not only in the external field but also in the

field induced by the magnetic moments of the superconducting granules. The relationship between the magnetization of superconducting granules and the magnitude of the total field in the intergranular medium was revealed in a series of works on the study of magnetic-transport effects in granular superconductors [48-58]. Further we apply the concept of effective field in the intergranular medium of a granular superconductor.

As the external field increases, Meissner currents circulate both through the intergranular boundaries ($\mathbf{J}_{MGB}$ currents) throughout the entire volume of the granular sample and within each superconducting granule ($\mathbf{J}_{MG}$ currents). They generate diamagnetic responses from the intergranular boundary subsystem and the granule subsystem, respectively, see the schematic representation in Fig. 4. The external field penetrates into the intergranular boundary subsystem at sufficiently small external field magnitudes (fractions of an Oersted) in the form of Josephson vortices [39]. For our case, in a field larger than about 12 Oe, the height of the ΔM_{GB} hysteresis loop becomes small, the diamagnetic response from the subsystem of intergranular boundaries is practically absent, and for the range of fields $H > 10$ Oe we should apparently speak either of the flow of Josephson vortices or simply of magnetic flux. At lower fields, one can operate with the magnetic moment from the $\mathbf{M}_{GB}$ intergranular boundary subsystem, the magnetic induction lines (dashed lines in Fig. 4) from which are closed outside the sample. The magnetic moments of the $\mathbf{M}_{GR}$ granules in fields $H < H_{1P}$ *are* determined only by the Meissner currents $\mathbf{J}_{MG}$. At $H > H_{1P}$, the Abrikosov vortices can penetrate many granules, located predominantly along the **H** direction; the vortices give a positive contribution to the total magnetization of the superconductor. The modulus of the $\mathbf{M}_{GR}$ vectors can be considered to decrease due to the contribution of the vortices. The magnetic induction lines from the $\mathbf{M}_{GR}$ magnetic moments (dashed lines in Fig. 4) should close not only outside the sample, but also through the intergranular boundaries, as shown in Fig. 4.

Proceeding from the described picture, in the intergranular medium the superposition of the external field **H** and field $\mathbf{B}_{ind}$ induced by the magnetic moments of $\mathbf{M}_{GR}$. Applied to the subsystem of intergranular boundaries, one can operate with the averaged or effective field $\mathbf{B}_{eff}$, and, $\mathbf{B}_{eff} = \mathbf{H} + \mathbf{B}_{ind}$. It is clear that $\mathbf{B}_{ind}$ depends on $\mathbf{M}_{GR}$, and since the magnetization of the subsystem of superconducting granules $\mathbf{M}_G$ is the sum of $\mathbf{M}_{GR}$ from all granules, this relation can be written as

$$\mathbf{B}_{ind} = \alpha \mathbf{M}_G$$

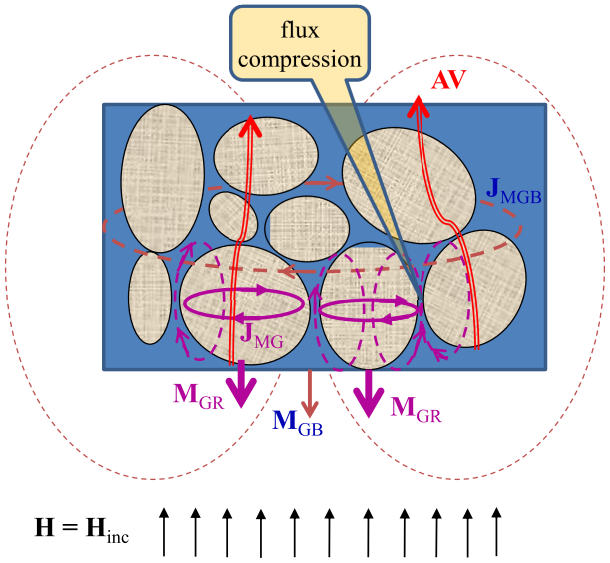

Fig. 4. Schematic representation of the mutual arrangement of the external field vectors **H** (increasing), Meissner currents $\mathbf{J}_{MGB}$, $\mathbf{J}_{MG}$, magnetic moments $\mathbf{M}_{GB}$, $\mathbf{M}_{GR}$ from the subsystem of intergranular boundaries (indices "MGB" and "GB") and granules (indices "MG" and "GR"). The magnetic induction lines from $\mathbf{M}_{GB}$ and $\mathbf{M}_{GR}$ are shown (dashed lines and highlighted in color). The location of Abrikosov vortices (AV) is also schematically represented.

or

$$\mathbf{B}_{ind}(H) = \alpha \mathbf{M}_G(H).$$

Here, the averaged proportionality factor α includes both the influence of demagnetizing factors of the granules and the effect of strong compression of the magnetic flux in the intergranular medium [51, 53-58]. With the mutual arrangement of the vectors $\mathbf{H}(H = H_{inc})$ and $\mathbf{M}_{GR}$, shown in Fig. 4, we can write the expression for the scalar value of the effective field in the form of

$$B_{eff} = H - \alpha M_G,$$

and, finally, operating with the magnetization of the granules $M_G(H)$, the following expression can be written down:

$$B_{eff}(H) = H - \alpha M_G(H). \qquad (4)$$

The expression (4) was used to analyze the field hysteresis of magnetoresistance and critical current, and based on numerous experiments, it was shown that the dimensionless parameter α has a rather large value, $\alpha \sim 10$-20 (with M_G measured in Gausses) [51, 53-58], which is an indication of magnetic flux densification in the intergranular medium.

Applied to the small magnetization hysteresis (lower inset of Fig. 1), the described concept of the effective field in the intergranular medium implies that the dependence of $M_{GB}(H)$ is a function of B_{eff}, i.e., $M_{GB}(B_{eff}) = f(H - \alpha M_G(H))$. It follows that not only the external field but also the magnetic moments of the granules are responsible for the decrease in the height of the $M_{GB}(H)$ hysteresis loop. From the data of Fig. 1 (lower inset) and Fig. 2 (upper inset) we can conclude that in the external field $H_{inc} = (12 \pm 1)$ Oe the value of ΔM_{GB} (at $H_{inc} = H_{dec}$) becomes very small. The magnitude of the effective field B_{eff} at $H_{inc} \approx 12$ Oe is equal to $B_{eff} \approx 12\ \text{Oe} - \alpha \cdot (-8\ \text{G})$. On the other hand, it was found above that at $H_{max} = 173$ Oe the small hysteresis is not evident in weak fields (range ±5 Oe). To estimate the effective field by expression (4) in the specified field range, we take the value $M = M_{Rem}(H_{max} = 173\ \text{Oe})$ roughly equal to 9 Gs and then we obtain $B_{eff} \approx 0 - \alpha \cdot 9$ G. Comparing the effective field moduli for the considered cases, we obtain

$$\left|12Oe - \alpha \cdot (-8G)\right| \approx \left|0Oe - \alpha \cdot 9G\right|.$$

We obtain $\alpha \approx 12$ from this expression. However, what is important here is not the fact of confirming the large value of the parameter α, but the fact that the external field plays a very weak role in the obtained equality. In other words, it is not the external field penetrating into the intergranular boundary subsystem, but the field induced by the magnetic moments of the superconducting granules that mainly contributes to the reduction of the magnetic response from the intergranular boundary subsystem.

Thus, taking into account that the subsystem of intergranular boundaries is in the field B_{eff}, for the total magnetization of the granular superconductor instead of expressions (2) and (3) we can write down

$$M(H) = M_{GB}(H - \alpha M_G(H)) + M_G(H), \qquad (5)$$

where the parameter a is sufficiently large ($\alpha > 10$).

The disappearance of the arch-shaped feature of the $M(H)$ dependence in the range of small fields at a certain value of the maximum applied field (Fig. 3 *a*) and the collapse of the small magnetic hysteresis loop are adequately explained within the framework of expression (5).

4. CONCLUSIONS

A detailed study of the magnetic hysteresis of the granular yttrium HTS system in different ranges of external fields allowed us to reveal the peculiarities of the disappearance of the small hysteresis loop. The arc-shaped feature in the region of weak fields, which is a characteristic feature of the $M(H)$ dependence of granular HTSs, becomes less pronounced as the maximum external applied field H_{max} increases and disappears at $H_{max} \approx 170$ Oe ($T = 78$ K). In this case, we can speak about the collapse of the small magnetic hysteresis. The observed behavior is explained by the interaction between the superconducting subsystems of granular HTS: granules and intergranular boundaries. The magnetic hysteresis in weak (up to ≈ 12 Oe at $T = 78$ K) fields is a response from the intergranular boundary subsystem, and this subsystem is in an effective field that is a superposition of the external field and the field induced by the superconducting granules. Thus, the behavior of the small hysteresis loop is explained within the framework of the model of flow compression in the intergranular medium. The subsystem of the intergranular boundaries, which is a Josephson medium (and is responsible for the observed small hysteresis), is formed by superconducting granules. At the same time, the influence of the magnetic moments of superconducting granules on the intergranular medium leads to a rather rapid (with increasing external field) disappearance of the small magnetic hysteresis under certain conditions. We can say that the subsystem of granules both generates and eliminates the magnetic response from the subsystem of intergranular boundaries.

FUNDING

The study was performed within the framework of the State Assignment of the Institute of Physics of the Siberian Branch of the Russian Academy of Sciences. The magnetic measurements were carried out on the equipment of the Center for Collective Use of the Federal Research Center "Krasnoyarsk Science Center of the Siberian Branch of the Russian Academy of Sciences".

REFERENCES

1. Ch. Yao, Y. Ma, *Science* **24**, 102541 (2021).
2. D.M. Gokhfeld, M. R. Koblischka, A. Koblischka-Veneva, *Phys. Met. Metallogr.* **121**, 936 (2020).
3. G. Wang, M. J. Raine, D. P. Hampshire, *Supercond. Sci. Technol.* **31**, 024001 (2018).
4. J. Huang, H. Wang, *Supercond. Sci. Technol.* **30**, 114004 (2017).
5. J. Zhang, H. Wu, G. Zhao, L. Han, Jun Zhang, *Nanomaterials* **12**, 4000 (2022).

6. A.P. Menushenkov, A. A. Ivanov, O. V. Chernysheva, I A. Rudnev, M. A. Osipov, A. R. Kaul, V. N. Chepikov, O. Mathon, V. Monteseguro, F. d'Acapito, *Supercond. Sci. Technol.* **35**, 065006 (2022).
7. S. Eley, A. Glatz, and R. Willa, *J. Appl. Phys.* **130**, 050901 (2021).
8. Y. Yeshurun, A. P. Malozemoff, A. Shaulov, *Rev. Mod. Phys.* **68**, 911 (1996).
9. A.M. Balagurov, L. G. Mamsurova, I. A. Bobrikov, To Thanh Loan, V. Yu. Pomjakushin, K. S. Pigalskiy, N. G. Trusevich, A. A. Vishnev, *JETP* **114**, 1001 (2012).
10. N. G. Trusevich. Yu. Gavrilkin, L. I. Trakhtenberg, *JETP* **137**, 356 (2023).
11. T. V. Sukhareva, V. A. Finkel, *JETP Lett.* **108**, 243 (2018).
12. V. A. Kashurnikov, A. N. Maksimova, I. A. Rudnev, A. N. Moroz, *Phys. Metals Metallogr.* **122**, 434 (2021).
13. M.R. Koblischka, S. P. Kumar Naik, A. Koblischka-Veneva, D. M. Gokhfeld, M. Murakami, *Supercond. Sci. Technol.*, **33**, 044008 (2020).
14. D.M. Gokhfeld, N. E. Savitskaya, S. I. Popkov, N. D. Kuzmichev, M. A. Vasyutin, D. A. Balaev, *JETP* **134**, 707 (2022).
15. D. A. Balaev, D. M. Gokhfeld, S. I. Popkov, K. A. Shaikhutdinov, L. A. Klinkova, L. N. Zherikhina, A. M. Tsvokhrebov, *JETP* **118**, 104 (2014).
16. D. A. Balaev, A. A. Dubrovskiy, S. I. Popkov, K. A. Shaikhutdinov, O. N. Mart'yanov, M. I. Petrov, *JETP* **110**, 584 (2010).
17. T. V. Sukhareva, V. A. Finkel', *Tech. Phys.* **55**, 66 (2010).
18. T. V. Sukhareva, V. A. Finkel', *Phys. Solid State* **52**, 452 (2010).
19. L. G. Mamsurova, N. G. Trusevich, K. S. Pigalskiy, A. A. Vishnev, S. K. Gadzhimagomedov, Z. K. Murlieva, D. K. Palchaev, A. S. Bugaev, *J. Phys. Chem. B.* **12**, 908 (2018).
20. A.A. Lepeshev, G. S. Patrin, G. Y. Yurkin, A. D. Vasiliev, I. V. Nemtsev, D. M. Gokhfeld, A. D. Balaev, V. G. Demin, E. P. Bachurina, I. V. Karpov, A. V. Ushakov, L. Y. Fedorov, L. A. Irtyugo, M. I. Petrov, *J. Supercond. Nov. Magn.* **31**, 3841 (2018).
21. I.A. Rudnev, A. I. Podlivaev, D. A. Abin, S. V. Pokrovskii, A. S. Starikovskii, R. G. Batulin, P. A. Fedin, K. E. Prianishnikov, T. V. Kulevoy, *Phys. Solid State* **65**, 379 (2023).
22. A.N. Maksimova, I. A. Rudnev, I. A. Kashurnikov, A. N. Moroz, *Phys. Solid State* **65**, 517 (2023).
23. D.M. Gokhfeld, S. V. Semenov, I. V. Nemtsev, I. S. Yakimov, D. A. Balaev, *J. Supercond. Nov. Magn.* **35**, 2679 (2022).
24. E. Taylan Koparan, A. Surdu, A. Awawdeh, A. Sidorenko, E. Yanmaz, *J. Supercond. Nov. Magn.* **25**, 1761 (2012).
25. C.P. Bean, *Rev. Mod. Phys.* **36**, 31 (1964).
26. C. Navau, N. Del-Valle, and A. Sanchez, *IEEE Trans. Appl. Supercond.* **23**, 8201023 (2013).
27. L. Ji, M. S. Rzchowski, N. Anand, and M. Tinkham, *Phys. Rev. B* **47**, 470 (1993)
28. M. Mahel', J. Pivarc, *Physica C* **308**, 147 (1998).
29. V. V. Val'kov, B. P. Khrustalev, *JETP* **80**, 680 (1995).
30. E.V. Blinov, Yu.P. Stepanov, K. B. Traito, L. S. Vlasenko, R. Laiho and E. Lahderanta, *JETP* **79**, 433 (1994).
31. D.M. Gokhfeld, *Phys. Solid State* **56**, 2380 (2014).
32. G.E. Gough, M. S. Colclough, D. A. O'Connor, E. Wellhoffer, N. McN. Alford, T. W. Button, *Cryogenics* **31**, 119 (1991).
33. J. Jung, M.-K. Mohamed, S. C. Cheng, J. P. Franck, *Phys. Rev. B.* **42**, 6181(1990).
34. F. Pėrez, X. Obradors, J. Fontcuberta, X. Bozec, A. Fert, *Supercond. Sci. Technol.* **9**, 161-175 (1996).
35. B. Andrzejewski, E. Guilmeau, C. Simon, *Supercond. Sci. Technol.* **14,** 904 (2001).
36. L. Burlachkov, A. E. Koshelev, V. M. Vinokur, *Phys. Rev. B* **54**, 6750 (1996).
37. F.F. Ternovskii, L. N. Shekhata, *JETP* **35**, 1202 (1972).
38. A. A. Elistratov, I. L. Maksimov, *Phys. Solid State* **42**, 201 (2000).
39. E.B. Sonin, *JETP Lett.* **47**, 415 (1988).
40. J. Paasi, A. Tuohimaa, J.-T. Eriksson, *Physica C* **259**, 10 (1996).
41. G. Ravikumar and P. Chaddah, *Phys. Rev. B.* **39**, 4704 (1989).
42. P. Chaddah, K. V. Bhagwat, and G. Ravikumar, *Physica C* **159** 570 (1989).
43. M. Zehetmayer, *Phys. Rev. B.* **80**, 104512 (2009).
44. R. Lal, *Physica C.* **470**, 281 (2010)
45. D.M. Gokhfeld, *J. Supercond. Nov. Magn.* **36**, 1089 (2023).
46. C. Böhmer, G. Brandstätter, H. W. Weber, *Supercond. Sci. Technol.* **10**, A1 (1997).

47. R. Liang, P. Dosanjh, D. A. Bonn, W. N. Hardy, A. J. Berlinsky, *Phys. Rev. B* **50**, 4212 (1994).
48. D. Daghero, P. Mazzetti, A. Stepanescu, P. Tura, *Phys. Rev. B* **66** (13), 11478 (2002).
49. D. A. Balaev, D. M. Gokhfeld, A. A. Dubrovskiĭ, S. I. Popkov, K. A. Shaikhutdinov, M. I. Petrov, *JETP* **105**, 1174 (2007).
50. D. A. Balaev, A. A. Dubrovskiĭ, K. A. Shaikhutdinov, S. I. Popkov, D. M. Gokhfeld, Yu. S. Gokhfeld, M. I. Petrov, *JETP* **108**, 241 (2009).
51. D.A. Balaev, S. I. Popkov, E. I. Sabitova, S. V. Semenov, K. A. Shaykhutdinov, A. V. Shabanov, M. I. Petrov, *J. Appl. Phys.* **110**, 093918 (2011).
52. A. Altinkok, K. Kilic, M. Olutas, A. Kilic, *J. Supercond. Nov. Magn.* **26**, 3085 (2013).
53. D.A. Balaev, S. V. Semenov, M. A. Pochekutov, *J. Appl. Phys.* **122**, 123902 (2017).
54. S.V. Semenov, D. A. Balaev, *Physica C* **550**, 19 (2018).
55. S.V. Semenov, D. A. Balaev, *J. Supercond. Nov. Magn.* **32**, 2409 (2019).
56. S.V. Semenov, A. D. Balaev, D. A. Balaev, *J. Appl. Phys.* **125**, 033903 (2019).
57. S.V. Semenov, D. A. Balaev, *Phys. Solid State* **62**, 1136 (2020).
58. S.V. Semenov, D. A. Balaev, M. I. Petrov, *Phys. Solid State* **63**, 1069 (2021).